Probability-dependent failure modes of slopes and cuts in heterogeneous cohesive soils

Van Den Eijnden, A. P.; Hicks, M. A.

DOI
10.1680/jgele.18.00043

Publication date
2018

Document Version
Accepted author manuscript

Published in
Geotechnique Letters

Géotechnique Letters **00**, 1–5, http://dx.doi.org/10.1680/geolett.XX.XXXXX

Probability-dependent failure modes of slopes and cuts in heterogeneous cohesive soils

A. P. VAN DEN EIJNDEN*, M. A. HICKS*

Improbable slope failure is addressed in the framework of reliability analysis of slopes in heterogeneous cohesive soils, as the small subset of realisations that fail without additional measures to trigger failure. The mode of these slope failures, located at the weak tail of the reliability curve, is demonstrated to differ significantly from the deterministic solution as well as the stochastic average solution found when shear strength reduction is applied to trigger slope failure. Subset simulation is applied to compute the probability-dependent difference in failure mode for a range of slopes down to very low levels of probability, which is required to properly account for the actual failure in predominantly safe slopes. The results demonstrate possible differences in the mode of failure when properly accounting for the uncertainty in spatial variability in a full probabilistic slope stability analysis, and highlight that caution may be needed when using the strength reduction method.

KEYWORDS: Embankments; Landslides; Numerical modelling; Shear strength; Slopes; Statistical analysis

LIST OF SYMBOLS

β	: slope angle
γ	: unit weight
μ_c	: mean shear strength
θ_1, θ_2	: horizontal, vertical scale of fluctuation
c	: (undrained) shear strength
d	: normalised depth of sliding surface
p_0	: target probability per subset
p_f	: probability of failure
CoV_c	: coefficient of variation of c
D	: ratio of domain height to slope height
F_G	: global factor of safety
$\widetilde{F}$	: factor of safety related to spatial variability
F_μ	: factor of safety based on mean strength
H	: slope height
N_c	: number of realisation passing threshold
E[.]	: expectation
MCS	: Monte Carlo simulation
RFEM	: random finite element method
ss	: subset
SuS	: subset simulation

INTRODUCTION

Numerical simulations of slopes generally involve several types of uncertainty. These include uncertainty in field and laboratory test data, uncertainty in the effect of translating these data into material parameters, uncertainty in the representativeness of the model (e.g. physical, geometrical), and inherent variability or randomness. Indeed, spatial variability is one of the important causes of uncertainty in slope stability analyses; it is an inherent variability that can be considered aleatory (Baecher & Christian, 2005) and its spatial nature requires a different approach than, for example, parametric uncertainty.

Over recent decades, spatial variability has found its place in geotechnical engineering (Vanmarcke, 1983; Christian et al., 1994; Phoon & Kulhawy, 1999; Uzielli et al., 2005), including slope reliability analysis. Modelled by random fields, spatial variability was first incorporated in (semi-) analytical models (Vanmarcke, 1980), before the development of the random finite element method (RFEM) where random field theory is combined with finite element analysis within a Monte Carlo simulation (MCS) framework (Griffiths & Fenton, 1993, 2004). RFEM has grown into an important probabilistic tool in geotechnical (e.g. slope stability) analysis, and has often involved parametric studies relating to the probability of failure p_f. However, few publications have focused on the resulting modes of failure or failure consequence (notable exceptions being Hicks et al. (2008); Hicks & Spencer (2010); Huang et al. (2013); Hicks et al. (2014); Zhu et al. (2015)). Data on such consequences are required when making the step from reliability analysis to risk assessment.

Whereas homogeneous slopes often have a well-established solution for the mode of failure and factor of safety (e.g. Taylor (1948)), stochastic simulations of heterogeneous slopes show a wide range of failure modes and a distribution of safety factors. Monte Carlo simulations indicated a range of correlation between factor of safety and mode of failure in Hicks et al. (2008, 2014) and Li et al. (2015), where the mode of failure was characterised by the width and volume of the sliding body in 3D analyses. Initial results suggested an inverse correlation (i.e. a negative coefficient of correlation) between the factor of safety based on the mean strength (F_μ) and the sliding volume/depth, although a lack of samples towards the tails of the distribution prevented more detailed investigation.

The application of subset simulation (Au and Beck, 2001) to slope stability problems within the framework of RFEM (Li et al., 2016) has enabled looking at the weak tail of the distribution in more detail. Indeed, investigating the relationship between factor of safety and mode of failure has corroborated earlier research, by showing a shallower mode of failure at low levels

Manuscript received. . .
Published online at www.geotechniqueletters.com
*Section of Geo-Engineering, Department of Geoscience & Engineering, Faculty of Civil Engineering and Geosciences, Delft University of Technology, Stevinweg 1, 2628 CN Delft, The Netherlands

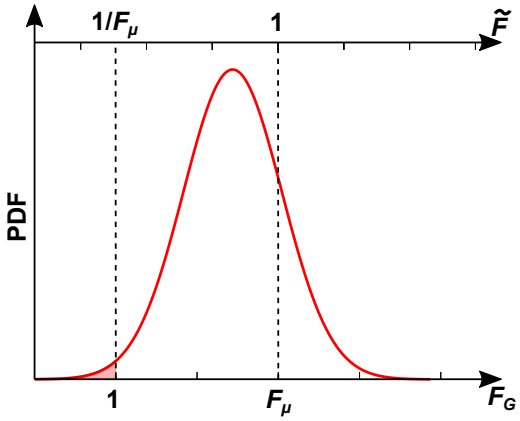

Fig. 1. Domain of interest for improbable slope failure events where $F_G < 1$ in the case of a deterministic F_μ. Shaded area represents probability of failure.

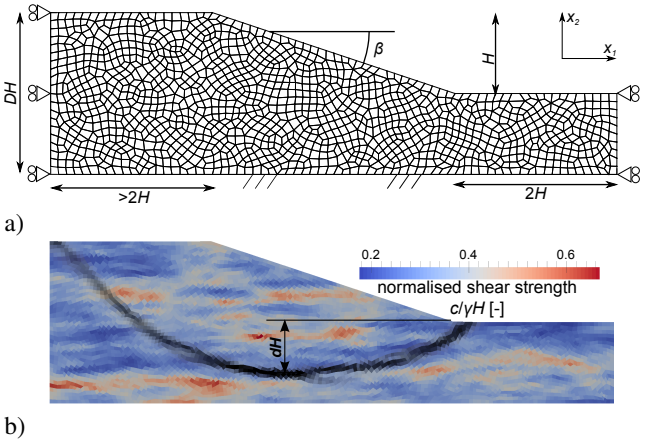

Fig. 2. Details of boundary value problem: (a) slope mesh comprising 1297 Q8 elements, with $D = 2$ and $\beta = 18.4°$ (the average mesh size is $0.1H$); (b) typical realisation with spatially varying c, for $CoV_c = 0.25$ and $\mu_c/\gamma H = 0.32$ (deviatoric strain contours, shown in black, indicating the sliding surface).

of failure probability (i.e. at high F_μ) (van den Eijnden & Hicks, 2017). These observations were made using RFEM for slopes of $45°$ in a cohesive material.

In this paper, the preferential failure mode as a function of slope angle, coefficient of variation and mean strength parameter, expressed in the context of the probability of failure, is investigated. Although more parameters influence the behaviour of such a model (e.g. scales of fluctuation, thickness of foundation layer), their variation is not considered here in order to keep the example concise.

IMPROBABLE SLOPE FAILURE

Shear strength reduction is applied to iteratively find the required strength reduction factor that brings the slope to failure. This realisation-specific global factor of safety F_G is here defined as the product of the factor of safety based on the mean strength F_μ and the variability factor of safety $\widetilde{F}$:

$$F_G = F_\mu \widetilde{F} \tag{1}$$

By this definition, $\widetilde{F}$ is the factor by which spatial variability reduces the effective strength compared to a homogeneous slope, with a smaller value for $\widetilde{F}$ meaning a weaker realisation and $\widetilde{F} = 1$ corresponding to a performance equal to a homogeneous slope. The distribution of $\widetilde{F}$ is determined by running a Monte Carlo simulation and normalising the computed values of F_G by the value of F_μ. Although F_μ can be stochastic, the limit case where F_μ is deterministic is considered here. This implies that slope failure will only occur in the subset of realisations for which $F_G < 1$, or $\widetilde{F} < 1/F_\mu$. This subset forms an improbable set of realisations at the weak tail of the distribution, especially when F_μ tends to be far from 1 in predominantly stable slopes (see Figure 1). Despite their small probability of occurrence, only the 'improbable slope failure' events in this subset are relevant in failure analysis. They form the only set of events that would actually occur in the case of slope failure, as opposed to all other events brought about by artificial strength reduction.

EXAMPLE OF PROBABILITY-DEPENDENT MODES OF SLOPE FAILURE

A slope of height H and angle β, founded on a layer of thickness equal to H, is considered. For the given geometry and boundary conditions (see Figure 2), an unstructured finite element mesh of 8-node quadrilateral elements is generated, upon which random fields of (undrained) shear strength c are superimposed using covariance matrix decomposition with local averaging (van den Eijnden & Hicks, 2017). The soil is modelled using a Tresca soil model. A lognormal distribution is assumed for c, characterised by a mean μ_c and coefficient of variation CoV_c. The spatial variability is characterised by an exponential correlation function, with horizontal and vertical scales of fluctuation $\theta_1 = 1.6H$ and $\theta_2 = 0.25H$, respectively.

First, MCS with 1000 realisations is performed on a $45°$ slope with $CoV_c = 0.25$ and normalised parameters $\mu_c/\gamma H = 0.32$ corresponding to $F_\mu = 1.74$, with γ being the unit weight. The normalised sliding depth d is determined using the K-means clustering method (Bishop, 2006), and plotted against F_G and $\widetilde{F}$ in Figure 3. The figure highlights the tendency for a generally weaker response in MCS compared to a homogeneous slope with the same mean strength, due to the sliding surface following the weakest path through the spatially variable soil. The scatter plot implies a weak correlation between F_G and d. Moving average filtering gives a first indication of the relationship between $\widetilde{F}$ and expected sliding depth (continuous line). The accuracy of the expected sliding depth can simply be improved by increasing the number of realisations, although MCS fails to efficiently address extremes of the solution range.

SUBSET SIMULATION

Subset simulation (Au and Beck, 2001) is used here to efficiently generate realisations at the weak tail of the distribution of $\widetilde{F}$, by generating realisations between subsequent thresholds of F_G. The threshold is lowered sequentially, in order to focus sampling on the tail of the distribution. Threshold values are determined by extrapolating the inferred probability function, aiming at a probability per subset of $p_0 = 0.10$, and realisations are generated until $N_c = 200$ have passed the lower threshold. Readers are referred to van den Eijnden & Hicks (2017) for further details on the performance-based subset simulation as applied in this paper, and validation against MCS. See Au and Wang (2014) for a general validation and discussion of subset simulation.

Figure 4 shows the results of a subset simulation of the case considered in Figure 3. The upper graph shows the calculated probability of failure p_f as a function of $\widetilde{F}$. The markers on the curve indicate the subset thresholds. The lower left graph shows the results for d per subset. The average and 5% and

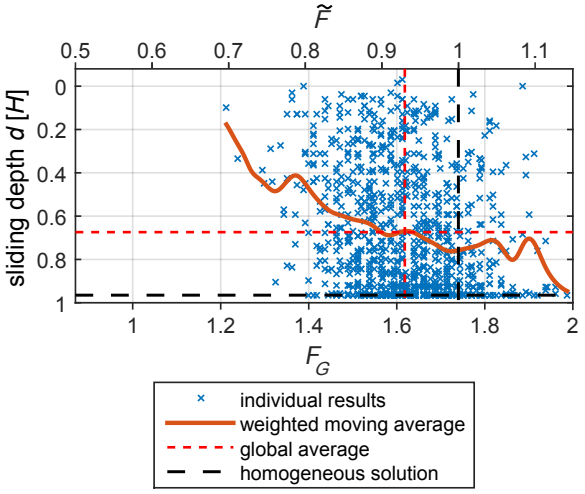

Fig. 3. Individual results of a 1000-realisation MCS, with local average trend for relative sliding depth d.

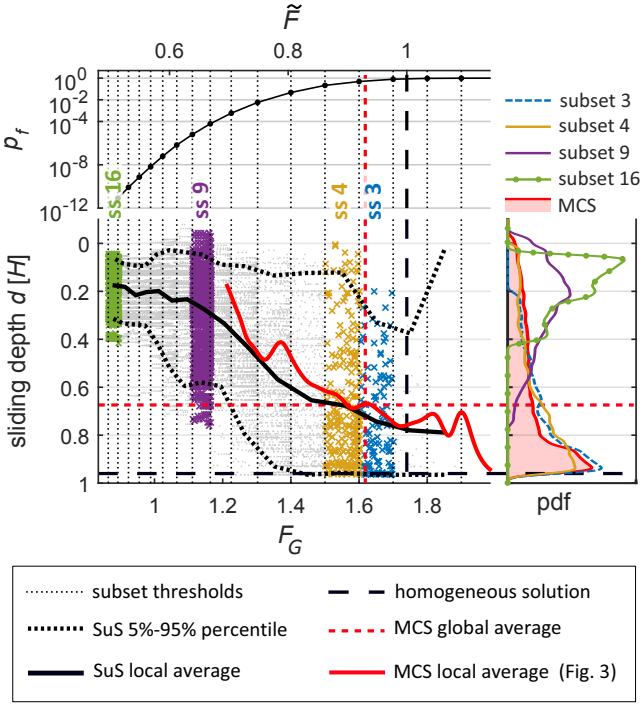

Fig. 4. Top-left: probability of failure against $F_G, \widetilde{F}$. Left: Sliding depths of individual realisations per subset with local average for a 45° slope with $CoV_c = 0.25$. Right; probability density functions of calculated sliding depth for subsets 3, 4, 9 and 16.

95% bounds per subset give an approximation of the expected sliding depth as a function of $\widetilde{F}$, which is a function of p_f.

For comparison, the local average of the MCS from Figure 3 is also given in Figure 4 and corresponds well to the average result of subset simulation in the range for which sufficient data points are available for reliable averaging (i.e. around the global average at $F_G = 1.62$), as do the scatter plots for the corresponding realisations. For lower values of $\widetilde{F}$ towards improbable slope failure at $\widetilde{F} < 1/F_\mu$, subset simulation provides a higher density of results relative to the total number of realisations, and thereby a more accurate estimation of the expected sliding depth. The lower right graph contains distributions of the subsets at $p_f \approx 0.5$ (subsets 3 and 4), $p_f \sim 10^{-4}$ (subset 9) and $p_f \sim 10^{-12}$ (subset 16). They show a change in the distribution of d with decreasing p_f, from a predominantly deep to a predominantly shallow mode of failure. This shift in distribution as a function of $\widetilde{F}$ (or its corresponding p_f) demonstrates once more the need to distinguish improbable slope failure from the bulk of results. This difference can further be expressed as the difference in expected sliding depth $\mathrm{E}[\Delta d]$ between the global and local average of the sliding depth:

$$\mathrm{E}[\Delta d] = \mathrm{E}[d] - \mathrm{E}[d|p_f] \tag{2}$$

with $\mathrm{E}[d]$ being the expected sliding depth obtained by shear strength reduction (i.e. not accounting for improbable slope failure) and $\mathrm{E}[d|p_f]$ being the expected sliding depth for improbable slope failure as a function of p_f. The difference in expected sliding depth will be used to characterise the difference between the overall results and improbable slope failure events.

PROBABILITY-DEPENDENT FAILURE MECHANISM

A set of 9×9 combinations of CoV_c and β is investigated using 10 independent subset simulations per combination with $N_c = 200$ failing realisations per subset. This has resulted in ~ 13 million realisations distributed over the solution space spanned by β, CoV_c and p_f in the ranges $[18.4° - 90°]$, $[0 - 0.40]$ and $[10^{-10} - 0.5]$, respectively. (Note that p_f is used as the leading parameter instead of $\widetilde{F}$, as its range is independent of β and CoV_c.) Parameters β and CoV_c are chosen at regular intervals, whereas the resulting p_f is slightly different between simulations as a result of Monte Carlo approximations of probability. To combine the results of repeated simulations, weighted moving average smoothing is applied to work out the probability-dependent sliding depth for each combination of β and CoV_c. Higher-order interpolation is then applied to obtain the expected sliding depth for the entire sampling space. These results in $\beta - CoV_c - p_f$ space can then be interpreted based on the relevant cross-sections or projections.

Figure 5 gives the expected sliding depth of the failing slope as a function of CoV_c for different slope angles. The homogeneous solution is indicated by the horizontal solid line. Probability levels ranging from $p_f = 0.5$ to $p_f = 10^{-10}$ indicate the evolution of the failure mode with failure probability. For homogeneous slopes with a deep mode of failure (i.e. $\beta <\approx 60°$) the homogeneous solution is the lower bound of all expected sliding depths. The expected sliding depth at $p_f = 0.5$ is very close to the global average sliding depth as calculated from MCS. Smaller probability levels show a consistently shallower sliding depth, migrating towards a shallow slope failure close to the toe of the slope at small enough probability levels. This migration is not very pronounced for low-angle slopes (see $\beta = 20°$, Figure 5a)), but reaches a relative difference with the global average (as approximated by $p_f = 0.5$) of over half the foundation layer depth for slopes with $30° <\approx \beta <\approx 60°$ for higher CoV_c. Note that at $\beta = 60°$, the probability-dependent expected sliding depth is, except for $CoV_c \approx 0$, independent of CoV_c. This is due to the angle of the slope being very close to the transition angle from deep to shallow failure in the homogeneous case (being between 53° and 60° (Taylor, 1948)), so that the introduction of small variations in strength is sufficient to trigger sliding surfaces anywhere between $d = 0$ and $d = 1$.

The relative difference in the expected sliding depth $\mathrm{E}[\Delta d]$ is presented as a function of β and CoV_c, by mapping $\mathrm{E}[\Delta d]$ for a series of constant p_f in Figure 6. Moderate levels of probability ($p_f \geq 0.05$) show a limited difference in sliding depth, with the maximum differences being for slopes around $\beta = 60°$ near the

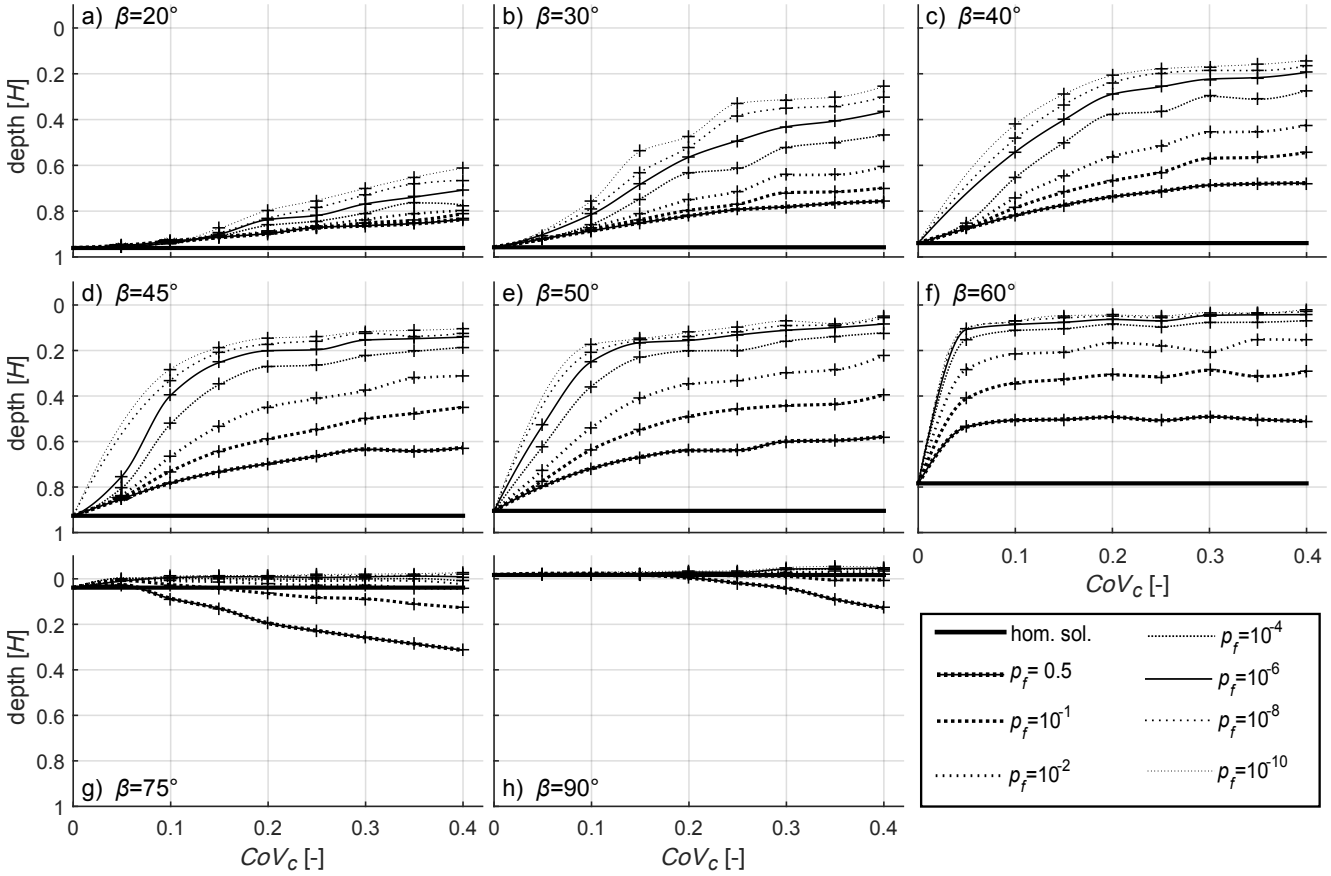

Fig. 5. Expected depth of sliding surface as a function of slope angle, failure probability and coefficient of variation of spatially variable shear strength.

transition angle from deep to shallow failure for homogeneous soils (Taylor, 1948). Smaller values of p_f show an increasing difference in failure mode, with the largest differences being obtained for $45^\circ - 60^\circ$ slopes with $CoV_c > 0.10$. These are the slopes that still have a predominantly deep mode of failure at high levels of failure probability.

The contours of $\widetilde{F}$ are given to indicate the factor by which the slope is weaker with respect to the homogeneous case based on the mean strength. This summarises the difference in calculated global factor of safety F_G between analyses of homogeneous and heterogeneous slopes.

Figure 6 demonstrates once more that the analysis of slope failure events at small levels of probability requires careful accounting of the effects of spatial variability. In addition to the difference between analysing failure using a deterministic analysis of a homogeneous slope and a Monte Carlo analysis of a heterogeneous slope by applying shear strength reduction, the mode of improbable slope failure is different from the bulk result of MCS and depends on the probability of failure under consideration.

CONCLUSIONS

Improbable slope failure has been introduced as the subset of realisations of a predominantly stable slope that fail without additional strength reduction. The mode of improbable slope failure can differ significantly from the global set of realisations obtained by shear strength reduction; a systematically shallower mode of failure is found for improbable slope failure when evaluating slopes at small probabilities of failure.

Results have shown that for studying slopes at small probabilities of failure, strength reduction can only be used to account for the uncertainty in the mean strength (i.e. the stochastic range of F_μ). For correctly predicting failure modes in spatially variable soils, slopes that fail without additional strength reduction have to be simulated. For structures with high global factors of safety, this requires advanced simulation techniques such as subset simulation.

ACKNOWLEDGEMENTS

This work is part of the research programme Reliable Dykes with project number 13864, which is partly financed by the Netherlands Organisation for Scientific Research (NWO). This work was carried out on the Dutch national e-infrastructure with the support of SURF Cooperative.

REFERENCES

Au SK and Beck JL (2001) Estimation of small failure probabilities in high dimensions by subset simulation. Probabilistic Engineering Mechanics **16(4)**: 263-277.

Au SK and Wang Y (2014) *Engineering risk assessment with subset simulation*. John Wiley & Sons Singapore Pte. Ltd., Singapore.

Baecher GB and Christian JT (2005) *Reliability and statistics in geotechnical engineering*. John Wiley & Sons Ltd., Chichester, England.

Bishop CM (2006) *Pattern recognition and machine learning*. Springer, New York, NY.

Christian JT, Ladd CC and Baecher GB (1994) Reliability applied to slope stability analysis. Journal of Geotechnical Engineering **120(12)**: 2180-2207.

van den Eijnden AP and Hicks MA (2017) Efficient subset simulation for evaluating the modes of improbable slope failure. Computers and Geotechnics **88**: 267-280.

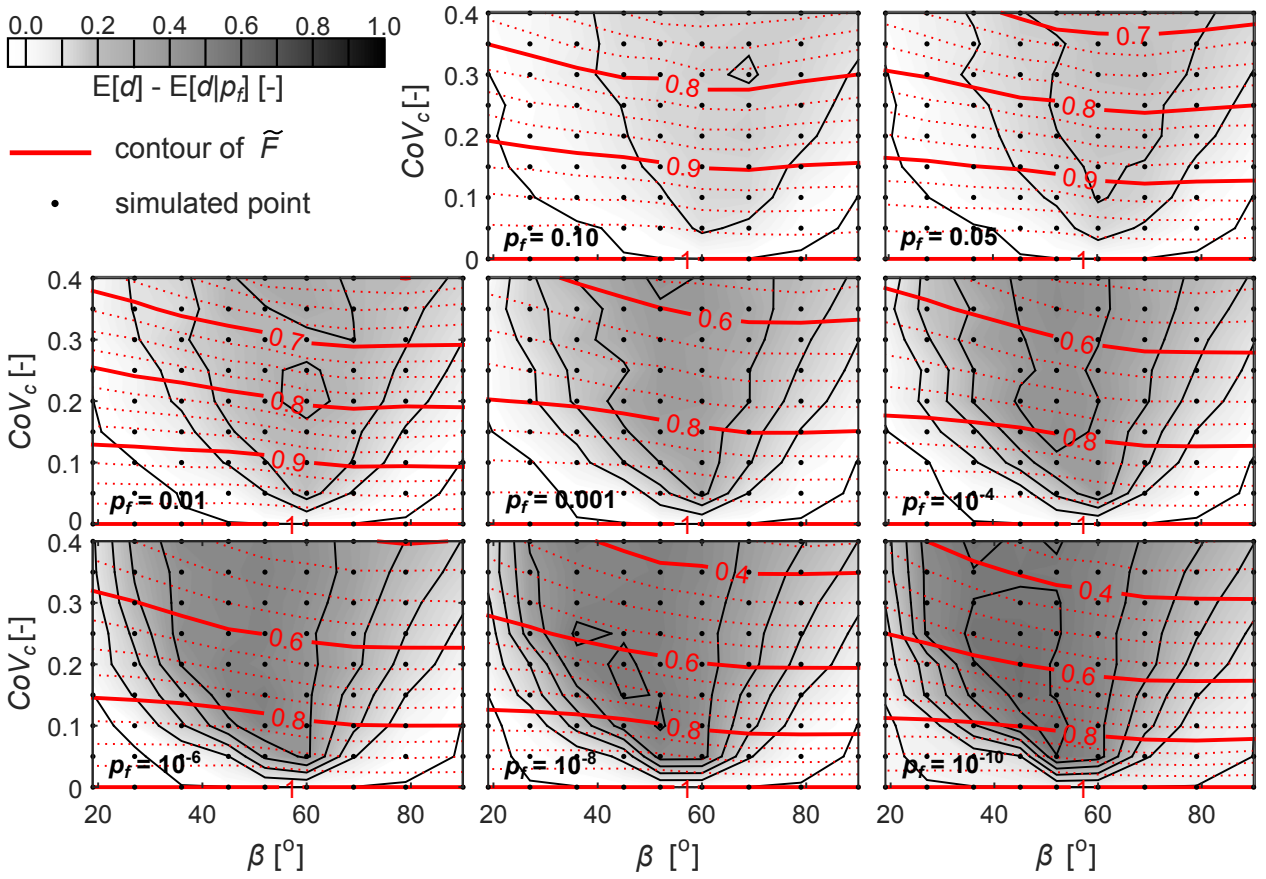

Fig. 6. Relative difference in the expected sliding depth $\mathrm{E}[\Delta d]$ at different levels of failure probability for $D = 2, \theta_1 = 1.6H, \theta_2 = 0.25H$.

Griffiths DV and Fenton GA (1993) Seepage beneath water retaining structures founded on spatially random soil. Géotechnique **43(4)**: 577-587.

Griffiths DV and Fenton GA (2004) Probabilistic slope stability analysis by finite elements. Journal of Geotechnical and Geoenvironmental Engineering **130(5)**: 507-518.

Hicks MA, Chen J and Spencer WA (2008) Influence of spatial variability on 3D slope failures. In *Proceedings of the 6th international conference on computer simulations in risk analysis and hazard mitigation, Cephalonia, Greece* (Brebbia CA and Beriatos E (eds)). pp. 335-342.

Hicks MA, Nuttall JD and Chen J (2014) Influence of heterogeneity on 3D slope reliability and failure consequence. Computers and Geotechnics **61**: 1198-1208.

Hicks MA and Spencer WA (2010) Influence of heterogeneity on the reliability and failure of a long 3D slope. Computers and Geotechnics **37(7-8)**: 948-955.

Huang J, Lyamin AV, Griffiths DV, Krabbenhoft K and Sloan SW (2013) Quantitative risk assessment of landslide by limit analysis and random fields. Computers and Geotechnics **53**: 60-67.

Li YJ, Hicks MA and Nuttall JD (2015) Comparative analyses of slope reliability in 3D. Engineering Geology **196**: 12-23.

Li DQ, Xiao T, Cao ZJ, Zou CB and Zhang LM (2016) Enhancement of random finite element method in reliability analysis and risk assessment of soil slopes using subset simulation. Landslides **13(2)**: 293-303.

Phoon KK and Kulhawy FH (1999) Characterization of geotechnical variability. Canadian Geotechnical Journal **36(4)**: 612-624.

Taylor DW (1948) *Fundamentals of soil mechanics*. John Wiley & Sons, Inc., New York, NY.

Uzielli M, Vannucchi G and Phoon KK (2005) Random field characterisation of stress-nomalised cone penetration testing parameters. Géotechnique **55(1)**: 3-20.

Vanmarcke EH (1980) Probabilistic stability analysis of earth slopes. Engineering Geology **16(1-2)**: 29-50.

Vanmarcke EH (1983) *Random fields: Analysis and synthesis*. MIT Press, Cambridge, MA.

Zhu H, Griffiths DV, Fenton GA and Zhang LM (2015) Undrained failure mechanisms of slopes in random soil. Engineering Geology **191**: 31-35.